PERSONALIZED IMPLANTS PRODUCED WITH SLM PROCESS

Grzegorz Bobik[1], Jarosław Żmudzki[1], Michał Bąk[2], Iwona Niedzielska[2], Marcin Adamiak[1], Paweł Popielski[3]

[1] Department of Engineering Materials and Biomaterials, Silesian University of Technology, 18a Konarskiego St., 44-100 Gliwice, Poland
[2] Department of Cranio-Maxillo-Facial Surgery, Medical University of Silesia, 20-24 Francuska St., 40-027 Katowice, Poland
[3] Institute of Biomedical Engineering, University of Silesia in Katowice, 39 Będzińska St., 41-200 Sosnowiec, Poland

Corresponding author: Grzegorz Bobik, grzegorz.bobik@polsl.pl

Abstract: Pure titanium is the material used to make personalized implants for maxillofacial surgery using selective laser melting (SLM). Not only the material but also the location of the screws has an influence on the transmission of occlusive loads through the bone structures, which in an unfavorable position may cause its loss. The aim of the study was to check the location and number of screws for transferring occlusive loads in the mandible model with the use of a titanium implant, thanks to the finite element analysis (FEA). After performing numerical tests, samples of CP-Ti were prepared and subjected to a tensile test and microscopic observations.
The FEA results showed that the implant is not subject to deformation and destruction, and the results of empirical studies are consistent with the numerical analysis.
Key words: titanium, mandible, dental implant, additive technology, SLM

1. INTRODUCTION

Mandibular implants in case of bone fractures are one of the most significant challenges in the field of bioengineering. Mandibular implants often include a temporomandibular joint (TMJ) caused by pathological changes related to occlusion dysfunctions, oncological changes, or congenital disabilities. A standard in the reconstruction of significant deficiencies in the mandible is the use of reconstruction plates [1-5], which, although they allow for fast connection of mandibular stumps, still make any prosthetic treatment difficult or impossible.
The development of CAD and SLM technologies introduces the possibility of producing personalized implants with new properties compared to casted and machined metals. Personalized implants are more advantageous in terms of the possibility of reconstructing the dentition and transferring the bite forces [6]. Porous titanium and polymers are indicated as attractive due to better fit with respect to bone stiffness [7]. Comparative studies [6] on ten rabbits treated implantologically in case of a broken mandible, showed that in terms of loosening the fixation screws and the condition of the bone tissue around the implants, better results were obtained in the group of 5 rabbits with individualized implants (porous Ti) compared to the group of 5 rabbits, with the use of reconstruction plates. On the other hand, there are known clinical cases of implant failure [8], which indicate a lack of knowledge about the strength properties.
The strength requirements for implants should result from a state of stress when transmitting bite forces. In simulations of the transmission of occlusal forces, the tested state of stress depends on the adopted load and support conditions for the mandible. Failures and discrepancies in the approach to modeling the transmission of bite forces were the motivation to verify the stress state in the implant material and the surrounding bone tissue and to try to optimize the implant.
The aim of the study was strength analysis and load-bearing ability of personalized large mandibular implants with condyle obtained with SLM.
The hypothesis of the study was that the SLM of pure titanium powder technology enables the optimization of mandibular implants while maintaining their load-bearing ability.

2. EXPERIMENTAL

2.1 3D model of the implant and bone

The bone model was made from CT images using Mimics software. Based on the pictures have been created a mask, and then had been transformed into a three-dimensional model. Purification of the artifacts from the model, models, transferred to NX Siemens, wherein split surfaces of the model to the muscle attachments and supports areas (Figure 1). Then created three variants of screws distribution in the implant: original with fewer screws and more screws.

The models prepared in this way, a TET10 element mesh was created, the total number of elements: 978402 elements.

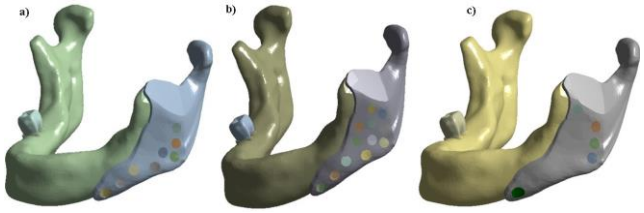

Fig. 1. Model geometry: a) Original version, b) Model with more screws, c) Model with fewer screws

For each attachment of the muscle was the united force of particular value and direction, shown in Table 1 and Figure 2.

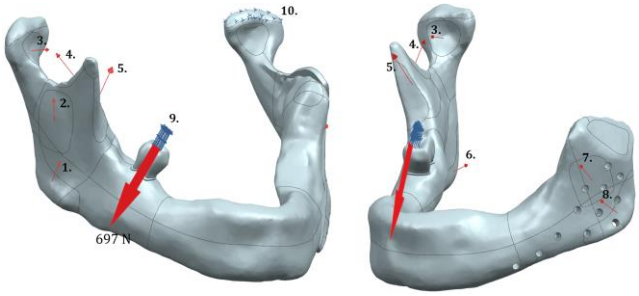

Fig. 2. Force directions and model support

Table 1. The value of forces [9]

Muscle	Force [N]
1. Right Superficial Masseter	196.3
2. Right Deep Masseter	82.1
3. Right Lateral pterygoid	81.4
4. Right Posterior Temporalis	156.6
5. Right Anterior Temporalis	221.5
6. Medial Pterygoid	170.7
7. Left Deep Masseter	16.32
8. Left Superficial Masseter	38.08
9. Model Support	Free in X, Y direction
10. Model Support	Fixed

For individual parts of the model, appropriate material properties were assigned, which were characterized by a different Young's modulus and Poisson's coefficient. The materials used during the numerical analysis are shown in Table 2.

Table 2. Material properties

Element	E	Poisson's Ratio
Cortical bone	14 000 MPa	0.3
Cancellous bone	800 MPa	0.3
Tooth	11 000 MPa	0.3
Periodontal ligament	20 MPa	0.48
Implant	96 000 MPa	0.36
Screws	96 000 MPa	0.36

2.2 SLM process and heat treatment

SLM technology was used to produce the samples, and the material used in the process was technically pure titanium. After finishing the process, the samples were heat treated.

SLM process parameters are as follows:

- Laser Power P – 100 W;
- Scan Speed SP – 700 mm/s;
- Energy Density E – 71.43 J/mm^3;
- Distance between scan lines HD – 0.8 mm;
- Layer thickness t – 0.025 mm;
- Laser diameter – 0.13 µm;
- Distance between scan points PD – 0.01 mm;
- Device: AM125 RENISHAW.

Parameters of the heat treatment process are as follows:

1. Draining the oven for 30 minutes.
2. Heating in an Argon 60 atmosphere for 2 hours.
3. I am soaking in Argon 60 atmosphere for another 2 hours.
4. Free cooling in an argon atmosphere for 1h 60 atmospheres.
5. Vacuum generation in a subsequent cooling stage (vacuum value $6.8 \cdot 10^{-3}$ [bar]).

2.3 Microscopy samples

Samples for light microscopy were ground on SiC papers of various grades, and then polished on a polishing cloth with the OP-U 4 µm reagent for 25 min. The final step was to digest the samples with Kroll's reagent for 15s. The samples prepared in this way were examined on the Zeiss Axio Observer light microscope.

2.4 Tensile test

The samples for the static tensile test were prepared by printing in the XZ plane, and the dimensions of the sample are shown in Figure 3. The experiment was performed with the MTS Criterion Model 43 testing machine. The tensile speed during the test was 0.5 mm / min.

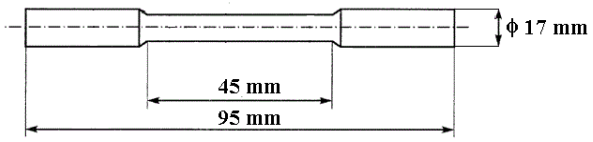

Fig. 3. Dimensions of the sample

3. RESULTS AND DISCUSSION

3.1 FEA analysis

The results of the FEA analysis show the Huber-Mises stress (H-M) for individual parts of the model: cortical bone, spongy bone, and titanium components - implant and screws.

In the case of the cortical bone (Figure 4), the highest

H-M stresses are concentrated around the lowest screw and oscillate around 64 MPa.

Table 3. Physiological range for bone structures [10]

The scope and type of load acting	800 MPa cancellous bone (MPa)	14000 MPa cortical bone (MPa)
Pathological underload (< 200 με)	<0.16 MPa	<1.4 MPa
Physiological range (200 <x< 2000 με)	0.16 – 2.5 MPa	1.4 - 28 MPa
Mild overload (2000 <x< 4000 με)	2.5 - 5 MPa	28 - 56 MPa
Pathological overload (4000 <x<10000με)	5 – 12.5 MPa	56 - 140 MPa
Bone fracture (> 10000 με)	>12.5 MPa	>140 MPa

According to Table 3, this is the extent to which the bone is heavily loaded over time and may cause bone lysis as well as bone weakness leading to fracture.
Comparing the stress distribution in the model with a reduced number of screws can be seen most uniform distribution. It is a situation in which the physiological load range occurs, and the H-M stress values do not exceed 28 MPa.
For other models, it is shown in the underload region ramus, and the stress value of H-M does not exceed 7 MPa.
Zones above 140 MPa are artifacts that arose during the analysis. The actual stress value in these places does not exceed 64 MPa.

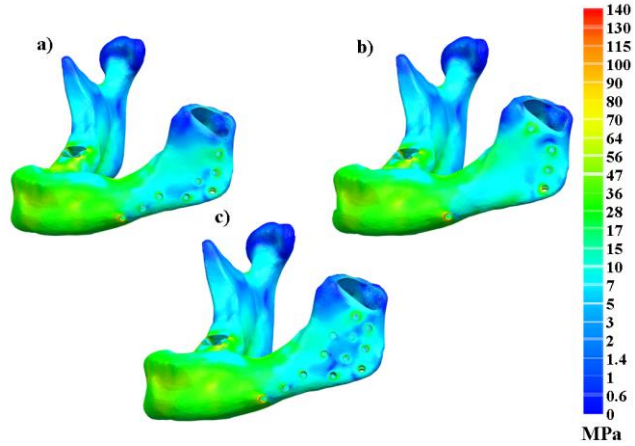

Fig. 4. H-M stress in cortical bone: a) original model, b) fewer screws model, c) more screws model

The stress analysis of H-M in the case of cancellous bone (Figure 5) maximum values were noted at the uppermost screws, but in the case of the original and a reduced number of screws, the area of the mandibular angle was highly activated.
Maximum stress value M-H observed during the test oscillates about 3.5 MPa, which are characterized by slight overload bone.
The areas of the highest activation occur in the original model and in the model with a reduced number of screws, but in the latter, the stress values are in the greater part in the range safe for the cancellous bone.

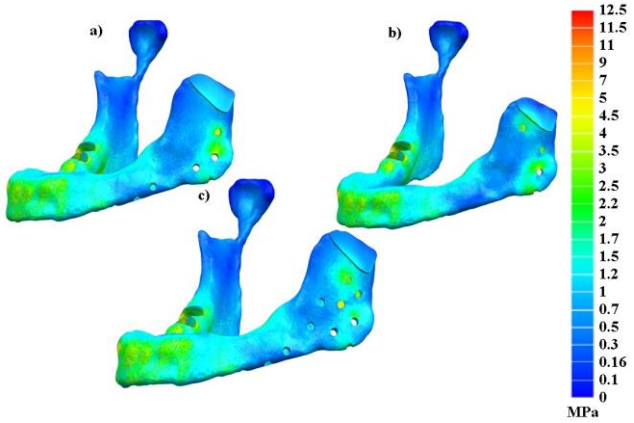

Fig. 5. H-M stress in cancellous bone: a) original model, b) fewer screws model, c) more screws model

Numerical analysis of H-M stresses occurring in the implant (Figure 6) showed that the stress zones do not exceed 130 MPa and are the same for all variants of the model. They occur in the neck of the implant and the inside of the implant with the angle of the mandible.

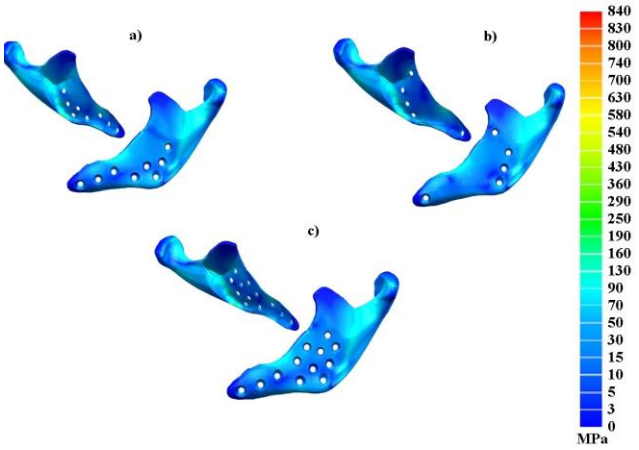

Fig. 6. H-M stress in implant: a) original model, b) fewer screws model, c) more screws model

3.2 Tensile test

Based on the graphs (Figure 7), the repeatability of the results for samples two up to five was observed, where the strength values for the samples amounted to approx. 800 MPa. Sample no. 1 showed slightly lower values, about 760 MPa. The obtained results show values higher than indicated by one of the literature sources [11] for pure titanium samples produced during the SLM process, where the obtained values indicate tensile strength without a clear yield point of (600÷750) MPa.

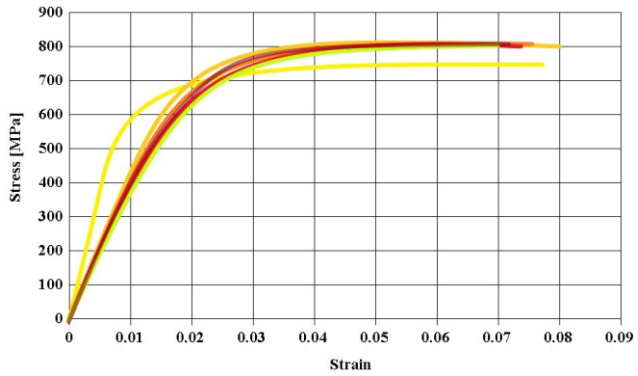

Fig. 7. Tensile stress-strain curves

3.3 Microscopic observations

The microscopic observations made it possible to detect α' structure and irregular pores (Figure 8 and 9). Moreover, due to the content of more closely spaced interfaces and higher dislocation density, the martensitic structure α′ is capable of obstructing the dislocation movement during deformation, which also contributes to an increase in tensile strength. It is therefore believed that a martensitic α' phase is formed to reduce the plasticity of the materials. However, their deterioration effect is considered to be very moderate, not as worse as that of iron alloys [12].

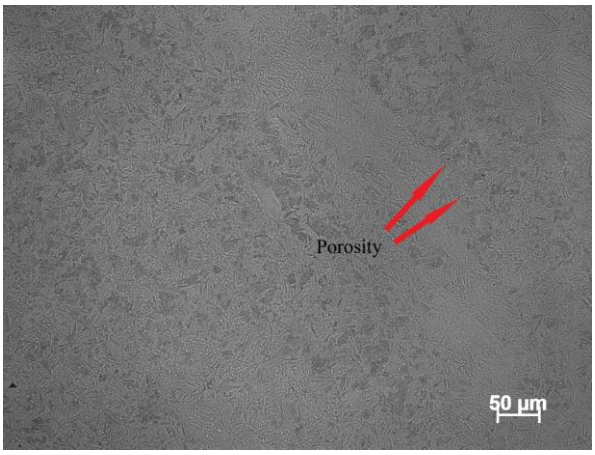

Fig. 8. Light microscope images of SLM-fabricated CP-Ti in XZ plane, X200

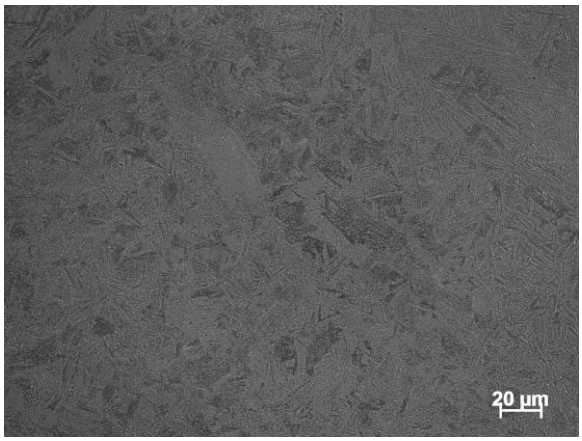

Fig. 9. Light microscope images of SLM-fabricated CP-Ti in XZ plane, X500

The previous findings may underestimate the maximum stress values, mainly when used to simplify the operation of occlusal forces only in the vertical direction [13-15]. An example is the clinical fracture of the implant in [8], in which the maximum stress was below 80MPa (stresses above this value are FEA artifact from mesh).

Also, the conditions of bilateral support in both joints [5] when transmitting the greatest lateral forces are not consistent with the fact that there is no joint support on the occlusal side as a result of moving the mandibular head out of the joint and gaining support on the tooth with food [16, 17]. It should be noted that resection patients with full muscular fitness may potentially achieve regular occlusal forces. The proposed in [4] introduction of a removable denture held on pins connected to the reconstruction plate increases the load on the reconstruction plate and the risk of fracture during the transmission of occlusal forces, as well as the risk of atrophy of cyclically overloaded bones around the fixation screws. The articular discs locally affect the distribution of condyle pressure, but the area of interest of this work was distant from the point of joint support. Hence, as in numerous studies [18-21], local effects may have been neglected.

The implant material strength requirements specified in [5] are approx. 170 MPa for a reconstruction plate with a thickness of 2 mm and a width of a dozen. Although the transfer of a unilateral lateral occlusion was simulated, both joints were rigidly supported. However, the value of the bite force that was to be generated by the adopted system of muscle activity was not given.

Meanwhile, studies of stress and biomechanics of the mandible clearly confirm the clinical assumptions [16, 17], relieve the joint working side.

Referring to the obtained results of numerical analysis, it can be concluded that reducing the number of screws used to stabilize the implant effectively improves the stress distribution in the cortical and spongy bone. Having a smaller area of bone underload prevents tissue loss, which is a major problem when treating a patient. The reduction in the amount of fabric destabilizes the system, which can cause serious problems. Also, the fixing points of the screws are subjected to the physiological range of load or are in a state of slight overload. A mild bone overload in these areas may result in the future build-up of bone tissue in this area and better stabilization of the implant [10].

The results of the numerical study also show that the stresses occurring in the implant during chewing do not exceed the limit values [11, 22-23]. The mechanical properties for CP-Ti used in SLM technology clearly show the safe range of stress and no damage to the implant.

Microscopic observation revealed a structure α' in the resulting samples - dendritic structure. The martensitic structure of α' allows reducing the formation and movement of dislocations, which results in greater tensile strength of the material. Additionally, it is possible to reduce the plasticity of the material [12, 24, 25]. Obtaining a 'structure made it possible to increase the tensile strength, as shown by the static tensile test. The values achieved by the material were close to 830 MPa, which was also shown in the literature [11, 24, 25]. Based on the numerical analysis and the tensile test, the thesis is confirmed that the implant will withstand occlusive stress and will not be deformed.

It should also be noted that the impact of the stress of the implant in the surrounding bone tissue is an important design criterion for implants [21, 26]. Paying attention to this criterion shall be certain modifications, such as the type of milling and the preparation of the powder, the use of controlled porosity, or adding other material to the titanium powder [12, 22, 23, 25,]. This results in the appropriate mechanical properties and safety of the patient during the use of the implant.

4. CONCLUSIONS

Studies have shown that the deployment of the implant stabilizing screws has a significant impact on the stress carried by the bony structures and areas underload. In addition, the tests of samples produced in the SLM technology proved that implants made of CP-Ti have sufficient mechanical properties and are safe to use. An additional advantage of Cp-Ti is the fact that it does not contain alloying additives, which, as in the case of alloys, may cause undesirable reactions of the body.

5. REFERENCES

1. Gullane, P. J., Havas, T. E., Holmes, H. H., (1986), *Mandibular reconstruction with a metal plate and myocutaneous flap*, The Australian and New Zealand journal of surgery, **56**(9), 701–706.

2. Li, B. H., Jung, H. J., Choi, S. W., Kim, S. M., Kim, M. J., Lee, J. H., (2012), *Latissimus dorsi (LD) free flap and reconstruction plate used for extensive maxillo-mandibular reconstruction after tumour ablation*, Journal of cranio-maxillo-facial surgery: official publication of the European Association for Cranio-Maxillo-Facial Surgery, **40**(8), e293–e300.

3. van Gemert, J, Holtslag, I, van der Bilt, A, (2015), *Health-related quality of life after segmental resection of the lateral mandible: Free fibula flap versus plate reconstruction*, Journal of Cranio-maxillo-facial Surgery: Official Publication of the European Association for Cranio-maxillo-facial Surgery, **43**(5), 658-662.

4. Kwon, I. J., Eo, M. Y., Park, S. J., Kim, S. M., Lee, J. H. (2016), *Newly designed retentive posts of mandibular reconstruction plate in oral cancer patients based on preliminary FEM study*, World journal of surgical oncology, **14**(1), 292.

5. Moiduddin, K., (2018), *Implementation of Computer-Assisted Design, Analysis, and Additive Manufactured Customized Mandibular Implants,* Journal of Medical and Biological Engineering, **38**, 744–756.

6. Lee, Y. W., You, H. J., Jung, J. A., Kim, D. W. (2018), *Mandibular reconstruction using customized three-dimensional titanium implant*, Archives of craniofacial surgery, **19**(2), 152-156.

7. Honigmann, P., Sharma, N., Okolo, B., Popp, U., Msallem, B., Thieringer, F. M. (2018), *Patient-Specific Surgical Implants Made of 3D Printed PEEK: Material, Technology, and Scope of Surgical Application*, BioMed research international, 2018, 4520636.

8. Huo, J., Dérand, P., Rännar, L.-E., Hirsch, J.M., Gamstedt, E. K., (2015), *Failure location prediction by finite element analysis for an additive manufactured mandible implant*, Medical Engineering & Physics, **37**(9), 862–869.

9. Gao, H., Li, X., Wang, C., Ji, P., Wang, C., (2019), *Mechanobiologically optimization of a 3D titanium-mesh implant for mandibular large defect: A simulated study*, Materials science & engineering. C, Materials for biological applications, **104**, 109934.

10. Thompson, S. M., Yohuno, D., Bradley, W. N., Crocombe, A. D., (2016)., *Finite element analysis: a comparison of an all-polyethylene tibial implant and its metal-backed equivalent*, Knee surgery, sports traumatology, arthroscopy: official journal of the ESSKA, **24**(8), 2560–2566.

11. Attar, H., Calin, M., Zhang, L.C., Scudino, S., Eckert, J., (2014), *Manufacture by Selective Laser Melting and Mechanical Behavior of Commercially Pure Titanium*, Materials Science and Engineering: A, **593**, 170-177.

12. Pehlivan, E., Roudnicka, M., Dzugan, J., Koukolikova, M., Králík, V., Seifi, M., Lewandowski, J.J., Dalibor, D., Daniel, M., (2020), *Effects of Build Orientation and Sample Geometry On the Mechanical Response of Miniature CP-Ti Grade 2 Strut Samples Manufactured by Laser Powder Bed Fusion*, Additive Manufacturing, **35**, 101403.

13. Wu, W. Z., Chen, Y. D., Cui, K. P., Qin, X. J., Wang, W. S., (2010), *Establishing 3D Mandible FEA Model via Clinical CT Images*, Applied Mechanics and Materials, 44–47, 1952–1956.

14. Hart, R.T, Hennebel, V. V., Thongpreda N., Van Buskirk, W. C., Anderson, R.C., (1992), *Modeling The Biomechanics of the Mandible: A Three-*

Dimensional Finite Element Study, Journal of Biomechanics, **25**(3), 261-286.
15. Wądłowski, P., Krzesiński, G., Gutowski, P., (2020), *Finite element analysis of mini-plate stabilization of human mandible angle fracture - a comparative study*, Acta of Bioengineering & Biomechanics, **22**(3), 165-186.
16. Okeson J. P., (1995), *Occlusion and functional disorders of the masticatory system*, Dental clinics of North America, **39**(2), 285–300.
17. Okeson J. P., (1981), *Etiology and treatment of occlusal pathosis and associated facial pain*, The Journal of prosthetic dentistry, **45**(2), 199–204.
18. Wang, H., Ji, B., Jiang, W., Liu, L., Zhang, P., Tang, W., Fan, Y., (2010), *Three-Dimensional Finite Element Analysis of Mechanical Stress in Symphyseal Fractured Human Mandible Reduced with Miniplates During Mastication*, Journal of Oral and Maxillofacial Surgery, **68**(7), 1585–1592.
19. Fernández, JR, Gallas, M, Burguera, M, Viaño, JM., (2003), *A three-dimensional numerical simulation of mandible fracture reduction with screwed miniplates*, Journal of Biomechanics, **36**(3), 329-337.
20. Korioth, T. W., Romilly, D. P., Hannam, A. G. (1992), *Three-dimensional finite element stress analysis of the dentate human mandible*, American journal of physical anthropology, **88**(1), 69–96.
21. Hsu, J. T., Huang, H. L., Tu, M. G., Fuh, L. J. (2010), *Effect of bone quality on the artificial temporomandibular joint condylar prosthesis*, Oral surgery, oral medicine, oral pathology, oral radiology, and endodontics, **109**(6), e1–e5.
22. Xu, W.C., Xiao, S., Chen, G., Liu, C., Qu, X. (2019), *Fabrication of commercial pure Ti by selective laser melting using hydride-dehydride titanium powders treated by ball milling*, Journal of Materials Science & Technology, **35**, 322-327.
23. Attar, H., Löber, L., Funk, A., Călin, M.F., Zhang, L., Prashanth, K.G., Scudino, S., Zhang, Y., Eckert, J. (2015), *Mechanical Behavior of Porous Commercially Pure Ti and Ti–TiB Composite Materials Manufactured by Selective Laser Melting*, Materials Science and Engineering A-structural Materials Properties Microstructure and Processing, **625**, 350-356.
24. Wysocki, B., Maj, P., Krawczyńska, A., Zdunek, J., Rożniatowski, K., Kurzydłowski, K.J., Święszkowski, W., (2016), *Microstructure and Mechanical Properties Investigation of CP Titanium Processed by Selective Laser Melting (SLM)*, Journal of Materials Processing Technology, **241**, 13-23.
25. Tao, Q., Wang, Z., Chen, G., Cai, W., Cao, P., Zhang, C., Ding, W., Lu, X., Luo, T., Qu, X., & Qin, M., (2020), *Selective laser melting of CP-Ti to overcome the low cost and high performance trade-off*, Additive manufacturing, **34**, 101198.
26. Bujtár, P, Sándor, GK, Bojtos, A, Szucs, A, Barabás, J., (2010), *Finite element analysis of the human mandible at 3 different stages of life*, Oral Surgery, Oral Medicine, Oral Pathology, Oral Radiology, and Endodontics, **110**(3), 301-309.

Received: May 25, 2020 / Accepted: December 20, 2020 / Paper available online: December 25, 2020 © International Journal of Modern Manufacturing Technologies